Carcinogenesis, 2015, Vol. 36, No. 10, 1213–1222

doi:10.1093/carcin/bgv112
Advance Access publication August 1, 2015
Original Manuscript

ORIGINAL MANUSCRIPT

MiR-17-92 cluster promotes hepatocarcinogenesis

Hanqing Zhu, Chang Han and Tong Wu*

Department of Pathology and Laboratory Medicine, Tulane University School of Medicine, 1430 Tulane Avenue SL-79, New Orleans, LA 70112, USA

*To whom correspondence should be addressed. Tel: +1 504 988 5210; Fax: +1 504 988 7862; Email: twu@tulane.edu

Abstract

MiR-17-92 cluster is an oncogenic miRNA cluster that is implicated in several cancers, although its role in hepatocarcinogenesis has not been clearly defined. In this study, we show that the miR-17-92 cluster is highly expressed in human hepatocellular carcinoma (HCC) tissues compared to the non-tumorous liver tissues by RT-PCR and *in situ* hybridization analyses. Increased miR-17-92 cluster expression in HCC tissues was further confirmed by analysis of the RNA-sequencing data of 319 patients available from the Cancer Genome Atlas (TCGA) Data Portal (https://tcga-data.nci.nih.gov/tcga/). To create an animal model that resembles enhanced miR-17-92 in the liver, we developed liver-specific miR-17-92 transgenic mice and the animals were treated with the hepatic carcinogen, diethylnitrosamine (DEN). We observed that the liver-specific miR-17-92 transgenic mice showed significantly increased hepatocellular cancer development compared to the matched wild-type control mice. Forced overexpression of the miR-17-92 cluster in cultured human hepatocellular cancer cells enhanced tumor cell proliferation, colony formation and invasiveness *in vitro*, whereas inhibition of the miR-17-92 cluster reduced tumor cell growth. By analyzing the miRNA and mRNA sequencing data from the 312 hepatocellular cancer patients available from the TCGA database, we observed that the expression levels of the miR-17-92 cluster members and host gene in the tumor tissues are negatively correlated with several target genes, including CREBL2, PRRG1, NTN4. Our findings demonstrate an important role of the miR-17-92 cluster in hepatocarcinogenesis and suggest the possibility of targeting this pivotal miRNA cluster for potential therapy.

Introduction

Hepatocellular carcinoma (HCC) is the fifth most prevalent cancer and third most frequent cause of cancer death (1,2). Common risk factors for HCC include chronic virus hepatitis B and C, alcoholic and non-alcoholic steatohepatitis and other causes of chronic liver diseases (3). The tumorigenic processes are complex and involve deregulation of multiple signaling pathways (4). The tumor is usually diagnosed at advanced stage which prevents curative therapies including surgical resection and liver transplantation, which are only applicable to patients at relatively early stages of tumor development (5). However, a majority of patients have advanced or unresectable disease at presentation which prevents curative treatments. Thus, HCC continues to represent a devastating human malignancy which requires further mechanistic investigations and more effective therapeutic interventions.

MicroRNAs (miRNAs) are a class of small non-coding RNAs (usually 19–24 nucleotides long) (6). They can target mRNAs through complementary binding at 3′UTRs with their seed sequences (7,8). Recent years, increasing studies have indicated the biological roles of miRNA in regulation of multiple biological processes. In light of cancer, miRNAs may function as oncogenes (oncomirs) or tumor suppressors and they may serve as potential biomarkers for cancer diagnosis, prognosis and therapeutic targets (9–11). MiR-17-92 cluster has been identified as oncogene (also known as *Oncomir-1*) (12). The miR-17-92 gene is located at the open reading frame of human chromosome 13, *C13orf25*. The host gene MIR17HG is non-coding, which can generate six mature miRNAs (miR-17, miR-18, miR-19a, miR-20, miR-19b and miR-92a) from the same primary transcript. MiR-17-92 has been shown to be highly expressed in various types of human cancers (including breast cancer, lung cancer, colon cancer and cholangiocarcinoma) (13–19). As for liver cancers, miR-17-92 is upregulated in cholangiocarcinoma (20) and miR-92a is reported to be upregulated in HCC (21). However, it remains unclear how miR-17-92 cluster is involved in hepatocellular carcinogenesis.

Received: April 9, 2015; **Revised:** July 6, 2015; **Accepted:** July 27, 2015

Abbreviations

DEN	diethylnitrosamine
HCC	hepatocellular carcinoma
miRNA	microRNA
mRNA	messenger RNA
PBS	phosphate-buffered saline
qRT-PCR	quantitative real-time polymerase chain reaction

The current study provides key evidence for an important oncogenic role of the miR-17-92 cluster in HCC. We show that miR-17-92 cluster is highly expressed in human HCC tissues and cells. By developing a novel liver-specific miR-17-92 transgenic mouse model, we observe that miR-17-92 expression in the liver enhances hepatocellular cancer development. The oncogenic role of the miR-17-92 cluster is further demonstrated by *in vitro* studies using cultured human HCC cells with miR-17-92 overexpression or inhibition. Analysis of the available miRNA and mRNA sequencing databases for HCC patients shows that the expression levels of the miR-17-92 cluster members and host gene in HCC tissues are negatively correlated with several target genes, including CREBL2, PRRG1 and NTN4. These findings demonstrate an important role of the miR-17-92 cluster in hepatocarcinogenesis.

Materials and methods

Materials

Minimum essential medium (MEM), Dulbecco's modified Eagle's medium and heat inactivated fetal bovine serum were purchased from Sigma (St Louis, MO). OPTI-MEM reduced serum medium, Lipofectamine™ 2000 reagent and puromycin were purchased from Invitrogen (Carlsbad, CA). Bronchial epithelial cell basal medium with supplemental growth factors in BEGM SingleQuot Kit was purchased Lonza (Walkersville, MD). The miR-17-92 cluster or miR-92a expressed and scrambled control lentiviral particles with enhanced green fluorescent protein were obtained from GeneCopoeia (Rockville, MD). Total RNA from human hepatocytes was purchased from Zenbio (Research Triangle Park, NC; Catalog - RNA-L10).

Cell culture

Five human HCC cell lines (Huh-7, Sk-Hep-1, Hep3B, HepG2, PLC/PRF/5) were utilized in this study. The HCC cell lines Sk-Hep-1 (ATCC® HTB-52™), Hep3B (ATCC® HB-8064™), HepG2 (ATCC® HB-8065™) and PLC/PRF/5 (ATCC® CRL-8024™) were obtained from the American Type Culture Collection (Manassas, VA) where the cell line were tested and authenticated by STR DNA profiling, mycoplasma detection, cell viability analysis and/or isoenzyme detection. Cells were cultured minimum essential medium containing 10% fetal bovine serum. Huh-7 (JCRB0403) was obtained from Japanese Cancer Research Resources Bank (Ibaraki City, Japan) where the cell line was tested and authenticated by STR DNA profiling and isoenzyme detection. Huh-7 cells were cultured in Dulbecco's modified Eagle's medium containing 10% fetal bovine serum. All cells were cultured in a humidified atmosphere of 5% CO_2 incubator at 37°C. The miR-92a or miR-17-92 cluster-overexpressed and scramble control stable cell lines were established by transduction with the corresponding lentiviral vector or miRNA-scrambled control lentiviral vector, followed by selection with media containing puromycin.

In situ hybridization for miRNA

In situ hybridization for miR-92a was performed in the formalin-fixed and paraffin-embedded tissue specimens surgically resected from patients diagnosed with HCC by using the MiRCURY LNA microRNA ISH Optimization Kit (Exiqon, Vedbaek, Denmark) with the approval of the Institutional Review Board. Briefly, 6-μm-thick paraffin sections were deparaffinized and treated with proteinase-K (15 μg/ml) at 37°C for 10 min. After dehydration, slides were incubated with 100 nM miR-92a locked nucleic acid probe (5′-DIG-ACAGGCCGGGACAAGTGCAATA-3′-DIG) at 50°C for 2 h, followed by stringent washes with 5× standard saline citrate, 1× saline sodium citrate and 0.2× saline sodium citrate buffers at 50°C; DIG blocking reagent (Roche) in maleic acid buffer containing 2% sheep serum at room temperature for 15 min; and alkaline phosphatase-conjugated antidigoxigenin (diluted 1:500 in blocking reagent; Roche) at room temperature for 2 h. Enzymatic development was performed by incubating the slides with 4-nitro-blue tetrazolium and 5-brom-4-chloro-3′-Indolylphosphate substrate (Roche) at 30°C for 2 h to allow formation of dark-blue 4-nitro-blue tetrazolium formazan precipitate, followed by nuclear fast red counterstain (Vector Laboratories, Burlingame, CA) at room temperature for 10 min. Slides were then dismantled in water, dehydrated in alcohol solutions and mounted with mounting medium (Vector Laboratories). Scrambled probe and U6 small nuclear RNA-specific probe were used as control. A standard four-point scale method was used to evaluate the staining intensity under microscope and the results were scored as 0 (negative), 1 (+), 2 (++) or 3 (+++) according to established criteria (22). Specifically, 3 (+++) indicates dark staining that is easily visible with a low power objective and involves > 50% of cells; 2 (++) indicates moderate darkly staining areas <50% of cells; 1 (+) indicates weak staining or pale staining in any proportion of cells not easily seen under a low power; 0 (negative) indicates no staining (showing none of the above staining). The same procedure was utilized to analyze the HCC tissue arrays (serial # LV2082, obtained from US Biomax, Rockville, MD). The tissue microarray consisted of 208 tissue core samples, including 94 cases of HCC, 5 cases of cancer adjacent normal hepatic tissue and 5 cases of normal liver tissue, each case with duplicate samples.

miRNA extraction and qRT-PCR

Cellular total RNA was isolated using Trizol reagent (Invitrogen). RNA from macrodissection-based formalin-fixed, paraffin-embedded patient tissues was isolated using an RNeasy formalin-fixed, paraffin-embedded Kit (Qiagen, Valencia, CA) following the manufacturer's protocol. Reverse transcription was performed by using miScript Reverse Transcription Kit (Qiagen). miScript SYBR Green PCR Kit (Qiagen) and miScript Primer Assays for six different miRs were used to amplify individual mature form of miR-17/18/19a/19b/20/92a on Bio-Rad C1000 Thermal Cycler. U6 small nuclear 2 (U6b) was used as the internal control. The Pre-miR-17-92 cluster gene was amplified by using the QuantiFast SYBR Green PCR Kit (Qiagen). GAPDH was used as the internal control. The pre-miR-17-92 cluster forward primer is 5′-CAGTAAAGGTAAGGAGAGCTCAATCTG-3′, reverse primer is 5′-CATACAACCACTAAGCTAAAGAATAATCTGA-3′. miRNA and mRNA expression was normalized to their corresponding internal control genes and relative change was calculated using the $2^{-\Delta\Delta CT}$ method.

Cell proliferation WST-1 assay

The cell proliferation reagent WST-1 (Roche) was used for quantitative determination of cellular proliferation according to the manufacturer's instruction. Briefly, the 2×10^3 cells were seeded onto each well of 96-well plates and cultured for 24 h to allow attachment. Then the medium was replaced with 100 μl fresh medium containing 1% fetal bovine serum or specific reagents as indicated and the cultures were continued for indicated days. For cell growth measurement, the cells were incubated in the presence of 10 μl/well WST-1 at 37°C and 5% CO_2 for 1 h. The absorbance of the samples was measured at 450 nm using an automatic ELISA plate reader (VersaMax Microplate Reader).

Colony-formation assay

About 1×10^3 cells were cultured in 10 cm dishes for 14 days to allow colony formation. Colonies were fixed in 100% methanol and stained with 0.1% crystal violet solution (Amersco, Solon, OH) for counting.

Cell invasion assay

The cell invasion assay was performed in matrigel-coated transwell chambers (BD Biosciences Discovery Labware, Bedford, MA). About 500 ul cell suspension (5×10^4 cells/ml) was added to each of the upper chambers. Cell culture medium containing 10% fetal bovine serum was added to each of the lower chambers as chemoattractant. After incubating cells at 37°C for 24 h, the cells on the upper surface of the membrane were removed with a cotton swab. The invading cells on the lower surface of

the membrane were fixed in 100% methanol and stained with Mayer's hematoxylin solution (IHC world, Woodstock, MD). Then the invading cells were counted under a microscope and for each chamber eight fields were randomly selected for counting.

Anti-miR transfection

miR-17/18/19a/19b/20/92a-specific anti-miR and scramble control miRNA (Qiagen, Valencia, CA) were transfected into cells by using Lipofectamine 2000 (Invitrogen, Carlsbad, CA) as per manufacturer's instruction. After transfection at indicated time periods, cells were analyzed for proliferation.

Generation of miR-17-92 cluster liver-specific transgenic mice

Alb-Cre mice (Strain Name:B6.Cg-Tg(Alb-cre)21Mgn/J, Stock Number:003574) and Loxp-miR-17-92-Loxp mice (Strain Name: C57BL/6-*Gt(ROSA)26Sor*$^{tm3(CAG-MIRN17-92,-EGFP)Rsky}$/J, Stock Number: 008517) were bought from Jackson Lab (Bar Harbor, ME) are bred together to generate miR-17-92 liver-specific transgenic mice. At 4 weeks, DNA was extracted from mice tail and subjected to polymerase chain reaction (PCR) genotyping of mice was performed using the following primers: Wild-type Forward 5′-CCAAAGTCGCTCTGAGTTGTTATC-3′, Wild-type Reverse 5′-GAGCGGGAGAAATGGATATG-3′, Transgenic Forward 5′-ACCTCC CCCTGAACCTGAAACA-3′, Transgenic Reverse: 5′-CAGTTTTACAAGGTGATGTTCTCTG-3′. PCR. All the mice used for experiments were maintained in the C57BL/6 background.

DEN-induced hepatocarcinogenesis model

miR-17-92 liver specific transgenic mice and wild-type control mice were used in this model. At 14 days postnatal age, the entire mouse litter received a single intraperitoneal injection of the genotoxic tumor initiator DEN (25 μg/g body weight; catalog no. N0756, Sigma, St Louis, MO; dissolved in 0.9% saline) which induces hepatocyte DNA damage through DNA adduct formation (23). Groups of seven male mice were used for the experiments. Mice were killed at 4, 8, 10, 12 months after DEN injection. At necropsy, terminal body weights, liver weights and liver morphology were evaluated. Livers were examined for the presence of liver tumors and sections of liver, liver tumors were fixed in 10% formalin and embedded in paraffin for histological examination. About 4 μm sections were made and stained with hematoxylin and eosin (H&E) or anti-Ki67 antibodies.

RNA-Seq data analysis

The Cancer Genome Atlas (TCGA) Data Portal (https://tcga-data.nci.nih.gov/tcga/, last accessed on September 16th, 2014) provides HCC patient mRNA sequence and miRNA sequence result. We utilized all the available level 3 data (319 HCC patient sample data), and imported the data into Subio platform Version 1.17 with Basic and Advanced Plug-ins (Kagoshima, Japan) for database management and data filtering, enrichment, clustering, find similar patterns and miRNA targets analysis.

Statistical analysis

Results are presented as mean ± SD or SEM from a minimum of three replicates. Differences between groups were compared using either Student *t* test or one-way analysis of variance (ANOVA). $P < 0.05$ was considered statistically significant. The analysis was performed using by SPSS 13.0 statistical software (IBM, Armonk, NY). For data from human samples, statistical significance between means was determined by the non-parametric Krustal–Wallis test.

Results

We first isolated RNA from formalin-fixed, paraffin-embedded tumor and liver tissues from 15 patients who underwent surgical resections for HCC and measured the levels of six mature miRNA (miR-17, miR-18a, miR-19a, miR-20a, miR-19b and miR-92a) of miR-17-92 cluster using quantitative RT-PCR. Compared to the adjacent nontumorous tissue, the tumor tissue showed significantly increased expression of all the six miRNAs. Among the six miRNAs, the expression level of miR-92a is the highest (Figure 1A). We also analyzed miRNA-sequencing data for HCC from TCGA data portal (https://tcga-data.nci.nih.gov/tcga/), which contains 319 miRNA-sequencing samples. Among a total number of 1047 miRNAs, 343 miRNAs are upregulated in tumors compared to non-tumor samples (Supplementary Table 1, available at *Carcinogenesis* Online), including miR-18a, miR-19a, miR-19b, miR-20a, all of which belong to miR-17-92 cluster, and ranked as top 100 miRNAs based on the expression level (Figure 1B). Next, we performed *in situ* hybridization using locked nucleic acid-modified probe against miR-92a in human HCC tissues. Ninety-four cases of human HCC tissue arrays were analyzed. We observed that the staining frequency and intensity of miR-92a are significantly higher in HCC cells (67.02% +++, 18.09% ++, 11.70% +, 3.19% –) compared to the non-tumorous liver tissues (0.00% +++, 0.00% ++, 20.00% +, 80.00% –) ($P < 0.01$) (Figure 1C). These findings document increased expression of miR-17-92 cluster in human HCC tissues.

We next performed experiments to evaluate the role of miR-17-92 cluster *in vivo*. We generated liver-specific miR-17-92 cluster transgenic mice by breeding the Loxp-miR-17-92-Loxp mice (which carry a loxP-flanked Neo-STOP cassette with a genomic DNA fragment encoding miR-17-92 gene) with the Alb-Cre mice (which carry Cre recombinase gene under the control of hepatocyte-specific Albumin Promoter) (Figure 2A). The offsprings were genotyped to confirm the removal of Neo-STOP cassette. A 6–25-fold increase of miR-17-92 cluster in liver tissue is confirmed by quantitative real-time polymerase chain reaction (qRT-PCR) at 4–8 weeks as well as at 10 months (Figure 2B and Supplementary Figure 1, available at *Carcinogenesis* Online). Thus far, we have successfully established the liver-specific miR-17-92 transgene mice. Next, we subjected the liver-specific miR-17-92 transgene mice and their matched wild-type controls to the hepatic carcinogen diethylnitrosamine (DEN)-induced hepatocarcinogenesis. The carcinogenic process was initiated by a single intraperitoneal injection of DEN at 25 μg/g body weight at postnatal day 14. Then the mice were killed at different time periods (4, 8, 10 months). At the 4-month period, only one out of four transgenic mice showed a small dysplastic focus, while the control mice showed no liver lesion. At the 8-month period, only few mice showed dysplastic foci or small tumor nodules, which were too few and two small to tally. At the 10-month period, all liver-specific miR-17-92 transgenic mice develop visible hepatocellular cancer, while control mice showed no tumor or very small tumor nodules (Figure 2B). As shown in Figure 2C, the average tumor number per mice is 5.29 ± 1.51 in the transgenic groups versus 0.86 ± 0.34 in the wild-type group ($P = 0.026$); the total tumor volume per mice is 1.86 ± 0.58 cm^3 versus 0.14 ± 0.01 cm^3 ($P = 0.029$); the maximum size of tumor in each mice is 132.86 ± 26.52 versus 15.51 ± 7.31 mm ($P = 0.002$). However, the liver/body weight ratio in the TG group is slightly higher compared to the WT group (9.26 ± 2.24 versus 5.66 ± 1.49), the difference is not statistically significant. Taken together, our data indicate that the liver-specific miR-17-92 transgenic mice developed significantly larger and more liver tumors compared to the wild-type mice (at 10 months after DEN injection). Under histological evaluation, the liver tumors in the miR-17-92 liver-specific transgenic mice comprise predominantly of HCC (85.71% HCC, 14.29% adenoma, 0.00% hyperplastic foci), while the liver lesions in the wild-type mice were predominantly of hyperplastic foci (0.00% HCC, 42.86% adenoma, 57.14% hyperplastic foci). The tumor progression status in the liver-specific miR-17-92 mice are generally more advanced than in the wild-type control mice (Figure 2D and E). No intrahepatic cholangiocarcinoma

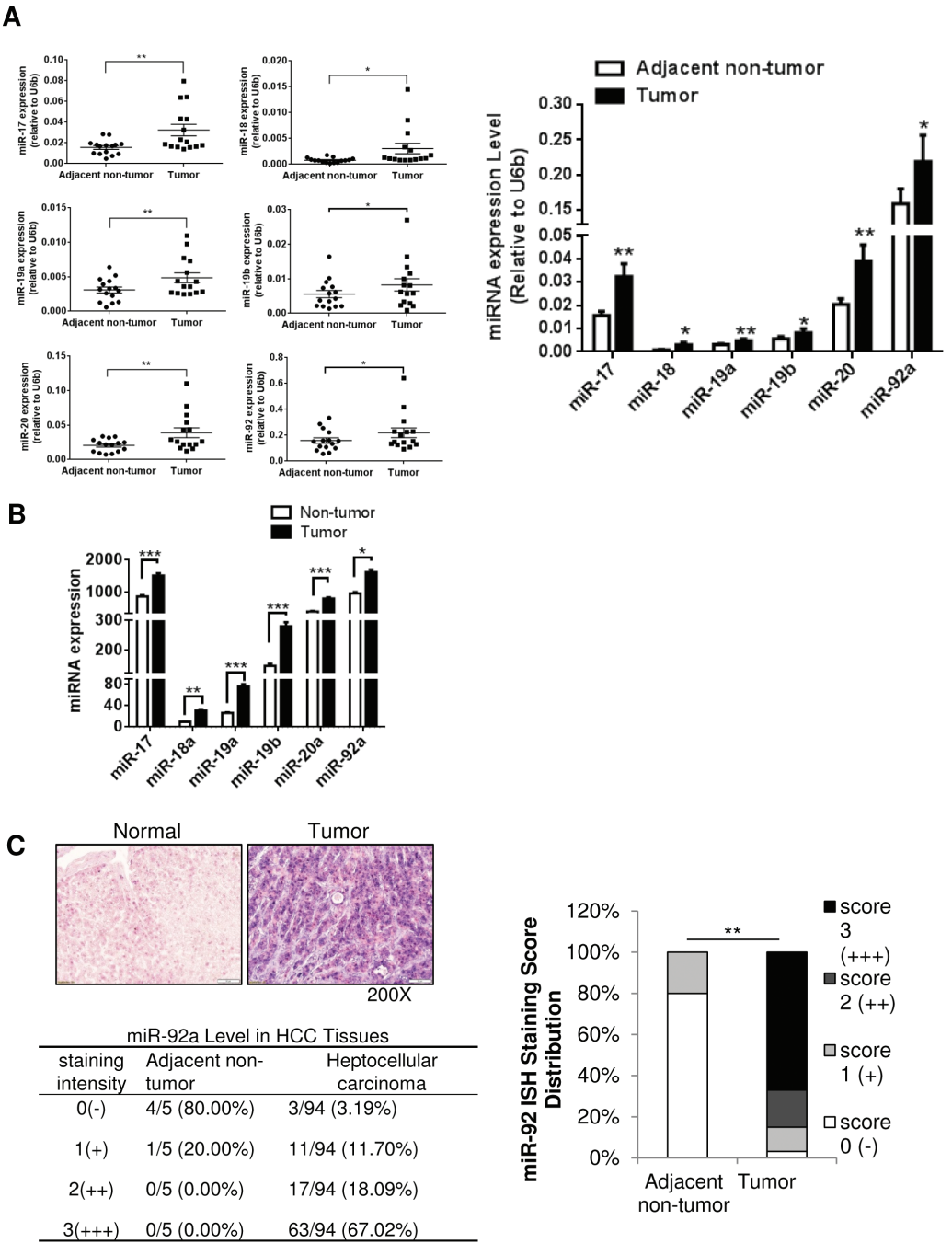

miR-92a Level in HCC Tissues

staining intensity	Adjacent non-tumor	Heptocellular carcinoma
0(-)	4/5 (80.00%)	3/94 (3.19%)
1(+)	1/5 (20.00%)	11/94 (11.70%)
2(++)	0/5 (0.00%)	17/94 (18.09%)
3(+++)	0/5 (0.00%)	63/94 (67.02%)

Figure 1. High expression of miR-17-92 cluster in HCC patient samples. (**A**) The individual miRNAs of miR-17-92 cluster are highly expressed in tumor tissues compared to non-tumor adjacent tissues from HCC patient sections. Total RNA are extracted from formalin-fixed, paraffin-embedded tissue sections for qRT-PCR. Individual miRNA expression levels are normalized to RNU6B (internal control). (*Left panel*) dot plots of individual miRNA expression levels normalized to U6b; (*Right panel*) bar graph of miR-17-92 cluster expression levels. *$P < 0.05$, **$P < 0.01$. (**B**) HCC patients miRNA-sequencing data were analyzed and compared between tumor and non-tumorous tissues. Individual mature miR-17-92 cluster miRNA expression is higher in tumor compared to normal (*$P < 0.05$, **$P < 0.01$, ***$P < 0.001$, one-way ANOVA). (**C**) *In situ* hybridization for mature miR-92a in HCC tissue array (*left upper panel*). Representative *in situ* hybridization images showing the expression of miR-92a in human HCC tissues and non-tumorous liver tissues. (Positive signals were shown as dark blue; nuclei were counterstained as red). Note positive miR-92a staining in HCC cells and negative staining in adjacent non-tumor areas; (*left lower panel*) Staining intensity score summary. (*Right panel*) Staining intensity score distribution in human HCC tissue arrays. There is a significant increase in tumor tissues compared to non-tumor tissues ($N = 94$, **$P < 0.01$ Krustal–Wallis non-parameter test).

is identified in these animals. The liver tissue sections from the miR-17-92 transgenic mice show more proliferative cells compared to that of the wild-type mice, as determined by the Ki67 immunostaining (Figure 2D). These findings demonstrate that overexpression of miR-17-92 cluster in the liver promotes hepatocellular cancer development, *in vivo*.

We further examined the levels of miR-17-92 cluster members in different human HCC cell lines and examined their effect on tumor cell growth. Compared to the human adult hepatocytes, all of the six miRNAs (miR-17/18/19a/19b/20/92a) are highly expressed in five HCC cell lines (Hep3B, PLC, HepG2, Huh-7 and Sk-hep-1), especially in PLC and Hep3B cells; the miR-17-92

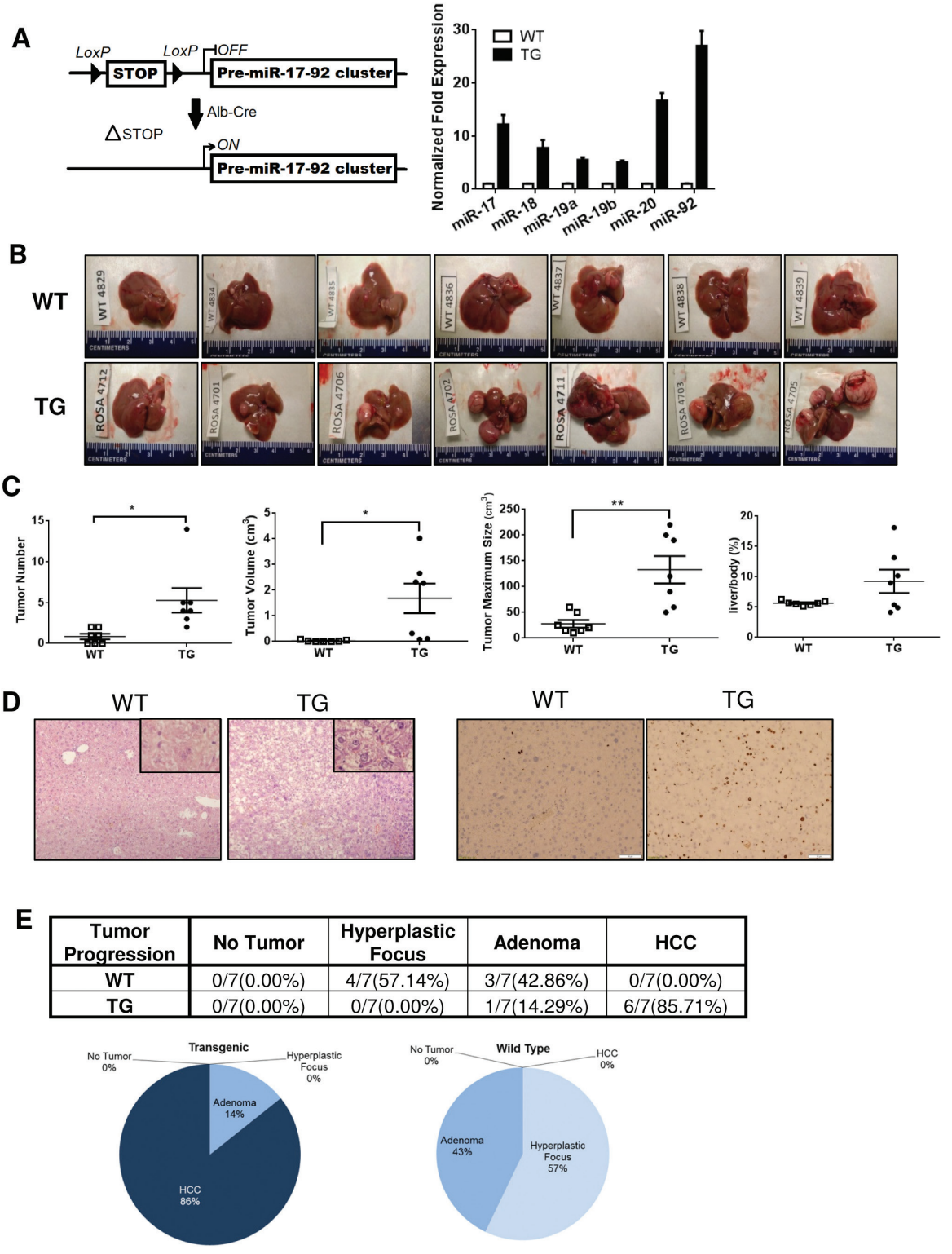

Tumor Progression	No Tumor	Hyperplastic Focus	Adenoma	HCC
WT	0/7(0.00%)	4/7(57.14%)	3/7(42.86%)	0/7(0.00%)
TG	0/7(0.00%)	0/7(0.00%)	1/7(14.29%)	6/7(85.71%)

Figure 2. Liver-specific miR-17-92 cluster transgenic mice promoted hepatocarcinogenesis. (**A**) (*Left panel*) Generation of liver-specific miR-17-92 cluster transgenic mice. In this model, the loxP-flanked stop element is deleted by Cre-mediated recombination. (*Right panel*) qRT-PCR result confirms high expression of miR-17-92 cluster in the liver-specific miR-17-92 cluster transgenic mice. Total cellular RNAs were extracted from liver tissues at 6–8 weeks (data are expressed as mean ± SEM, $P < 0.05$ for each miRNA). (**B**) Gross photograph of the liver of DEN-treated mice from both groups. (**C**) The liver-specific miR-17-92 cluster transgenic mice show significantly increased tumor burden compared to the matched wild-type control mice. Parameters of the tumor burden include (*from Left to Right*) liver tumor incidence, total liver tumor volume per mice, maximum tumor size, and liver/body weight ratio (%). Data are mean ± SEM, $N = 7$, $^{*}P < 0.05$, $^{**}P < 0.01$). (**D**) Immunohistochemical staining of the liver tissues from wild type and liver-specific miR-17-92 cluster transgenic mice. (*Left panel*) hematoxylin and eosin (H&E) stained tissues (100×) (the insert shows partial section from the same slide at 400×). (*Right panel*) Ki-67 stained tissues. (**E**) Classification of liver lesions based on histopathological evaluation. The data were from wild type and liver-specific miR-17-92 cluster transgenic mice 10 months after DEN treatment. The liver-specific miR-17-92 cluster transgenic mice show higher grade of liver tumors.

miRNAs are all in very low levels in human adult hepatocyte (HH). Similar to the results in human HCC tissue samples and in the liver tissues from the miR-17-92 transgenic mice, among the six mature miRNAs, miR-92a is the most abundant (Figure 3). We then constructed human HCC cell lines with stable overexpression of miR-17-92 by infecting the parental cell line (Huh-7 and Sk-hep-1) with lentivirus particles carrying the miR-17-92 gene or the scrambled control miRNA as control [these vectors also carry the enhanced green fluorescent protein gene (EGFP) under the control of the same promoter]. High infection efficiency was confirmed by the expression of EGFP in nearly all transduced cells. Successful overexpression of miR-17-92 cluster in the lentivirus stably transduced cells was verified by qRT-PCR. As shown in Figure 4A, overexpression of the miR-17-92 cluster significantly increased the growth of HCC cells *in vitro*. MiR-17-92 cluster overexpression also enhanced HCC cell invasiveness and colony-formation efficiency (Figure 4B and C). In contrast, inhibition of miR-17-92 cluster (via anti-miRs transfection) decreased tumor cell proliferation (Supplementary Figure 2, available at *Carcinogenesis* Online). In separate experiments, we observed that overexpression of miR-92a also enhanced HCC cell proliferation, colony formation and invasiveness (Figure 5). Taken together, these data document an important role of miR-17-92 cluster in HCC cell growth.

TCGA data portal contains large set of RNA sequence data of different types of cancer with clinical information. We analyzed all the available level 3 sequencing data of HCC patients from this database, which included the data from 319 HCC patients (all 319 patients had miRNA-seq data; 312 of 319 patients had matched RNA-seq data). Utilizing the Subio platform, we also made comparison between mRNA and miRNA sequencing result combined with seed sequence prediction from several online websites, including TargetScan (http://www.targetscan.org/) (24), PicTar (http://pictar.mdc-berlin.de/) (25–27) and Miranda (http://www.microrna.org/microrna/) (28). This approach allowed us to identify highly correlated miRNA-Target pairs (listed in Figure 6A and Supplemental Table 2, available at *Carcinogenesis* Online). CREBL2, EXPH5, NTN4, MYLK, PRRG1, ESR1 are highly possible targets of the miR-17-92 cluster, as they not only are predicted targets based on binding sequence but also show an expression pattern negatively correlated with the respective miRNAs in the tumor and non-tumor samples (Pearson Correlation) (Figure 6B). Given that

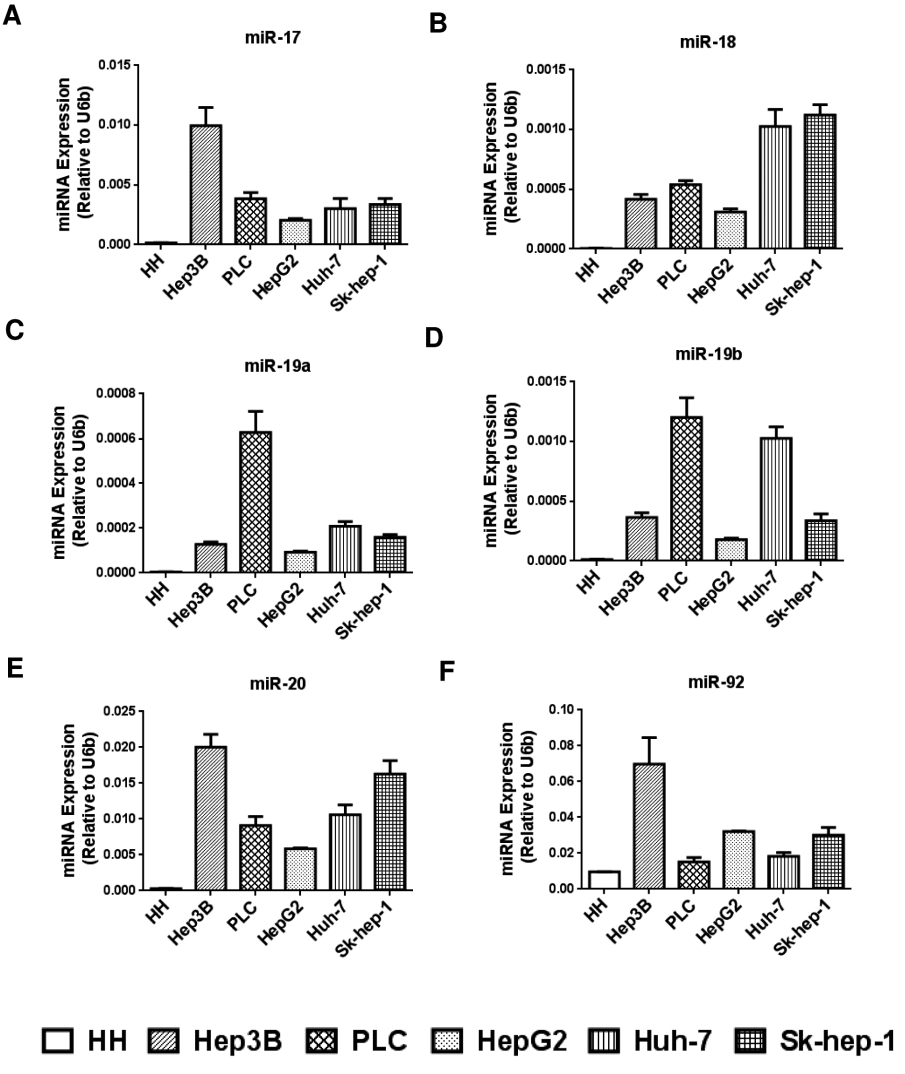

Figure 3. High expression of miR-17-92 cluster in human HCC cell lines. qRT-PCR for mature miRNA in miR-17-92 cluster in human adult hepatocytes (HH) and five different human HCC cell lines (Hep3B, HepG2, PLC, Huh-7, Sk-Hep-1). Total cellular RNAs were extracted for qRT-PCR. Each individual miRNA expression levels are normalized to RNU6B (internal control) ($n = 3$).

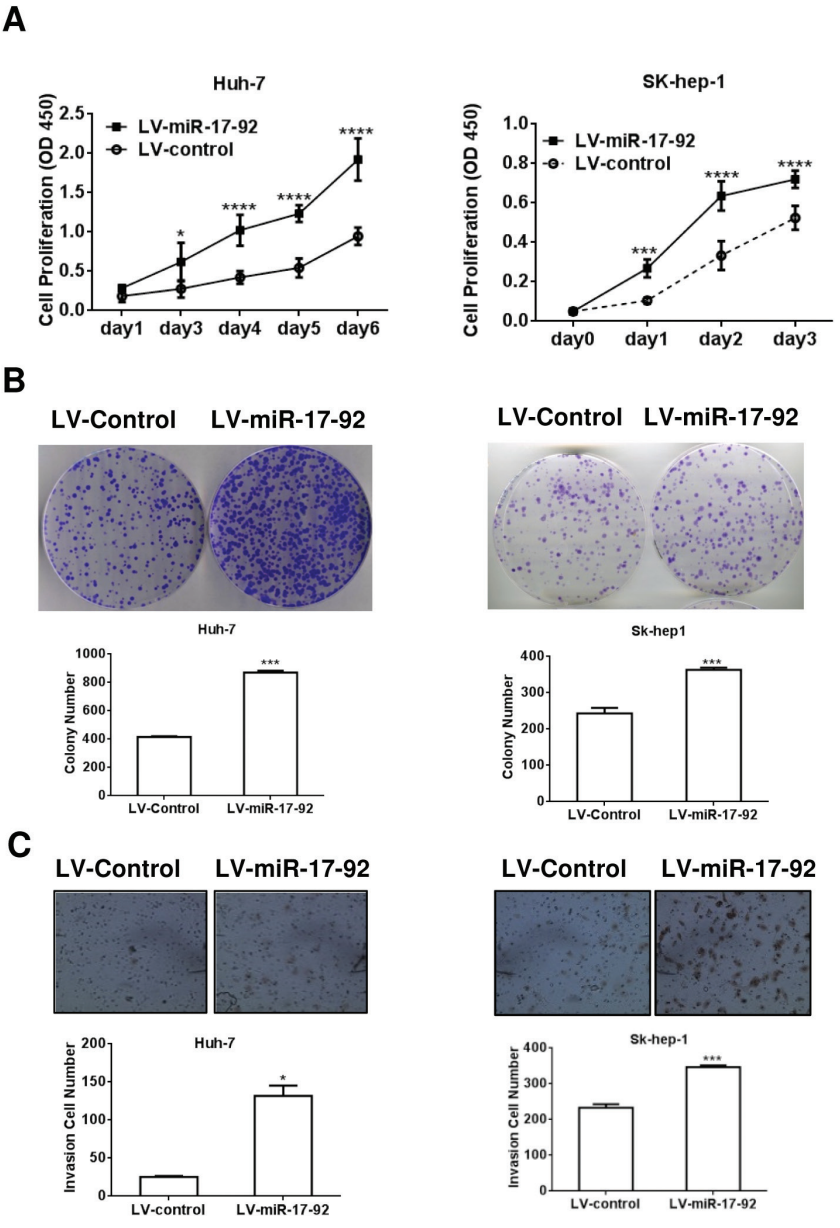

Figure 4. MiR-17-92 cluster promotes HCC cell growths *in vitro*. Human HCC cells (Huh-7 and Sk-Hep-1) were infected with miR-17-92 cluster lentivirus and miRNA scrambled control lentivirus, respectively. The stably transduced cells were analyzed for proliferation, colonogenic potential and invasion ability as described in the Materials and Methods section. (**A**) MiR-17-92 cluster over-expression promotes HCC cell growth. Cell growth curves of human HCC cells (Huh-7 and Sk-Hep-1) stably transduced with miR-17-92 cluster lentivirus (indicated as LV-miR-17-92) or scrambled control (indicated as LV-control) (*$P < 0.05$, ***$P < 0.001$, ****$P < 0.0001$). (**B**) MiR-17-92 cluster overexpression enhances HCC cell colony formation. The numbers of colonies were counted after 14 days. (*Upper panel*) Representative images showing colonies formed in cell culture dishes. (*Lower panel*) Average colony formation efficiency (the data is presented as mean ± SEM, ***$P < 0.001$). (**C**) MiR-17-92 cluster over-expression promotes HCC cell invasion. (*Upper panel*) Representative images showing migrated cells staining by Hematoxylin. (*Lower panel*) Average numbers of the invaded cells (the data are presented as mean ± SEM, *$P < 0.05$, ***$P < 0.001$).

MIR17HG is the host gene for the miR-17-92 cluster, we further analyzed its expression level to determine whether there might be a correlation between MIR17HG and the other genes from the RNA-seq database. We observed that the average expression of MIR17HG gene in HCC tumor is significantly higher than non-tumor groups ($P < 0.0001$) (Figure 6C), which is in accordance with increased miR-17-92 cluster members as shown in Figure 1 by qRT-PCR and ISH analyses. By comparing the expression patterns of MIR17HG and all other genes, we identified a list of genes whose expression pattern is negatively correlated with MIR17HG in the tumor and non-tumorous liver tissues (Supplementary Table 3, available at *Carcinogenesis* Online). We noticed that most of the identified genes are also targets of at least one miRNAs in miR-17-92 cluster. The most correlated targets (correlation –1 to –0.3) from that list are shown in Figure 6D; the expression levels of those genes are significantly downregulated (by threshold >1.5-fold) in the tumor (compared to the non-tumorous liver tissues). It is notable that several targets identified by miRNA-target pair analysis, including CREBL2, PRRG1 and NTN4, are also among the downregulated targets of the MIR17HG host gene. Based on these findings, we sought to further determine whether the expression of any of these targets might correlate with the patients' clinical outcomes. To this end, we extracted the clinical information from the database and analyzed the survival data; we grouped all

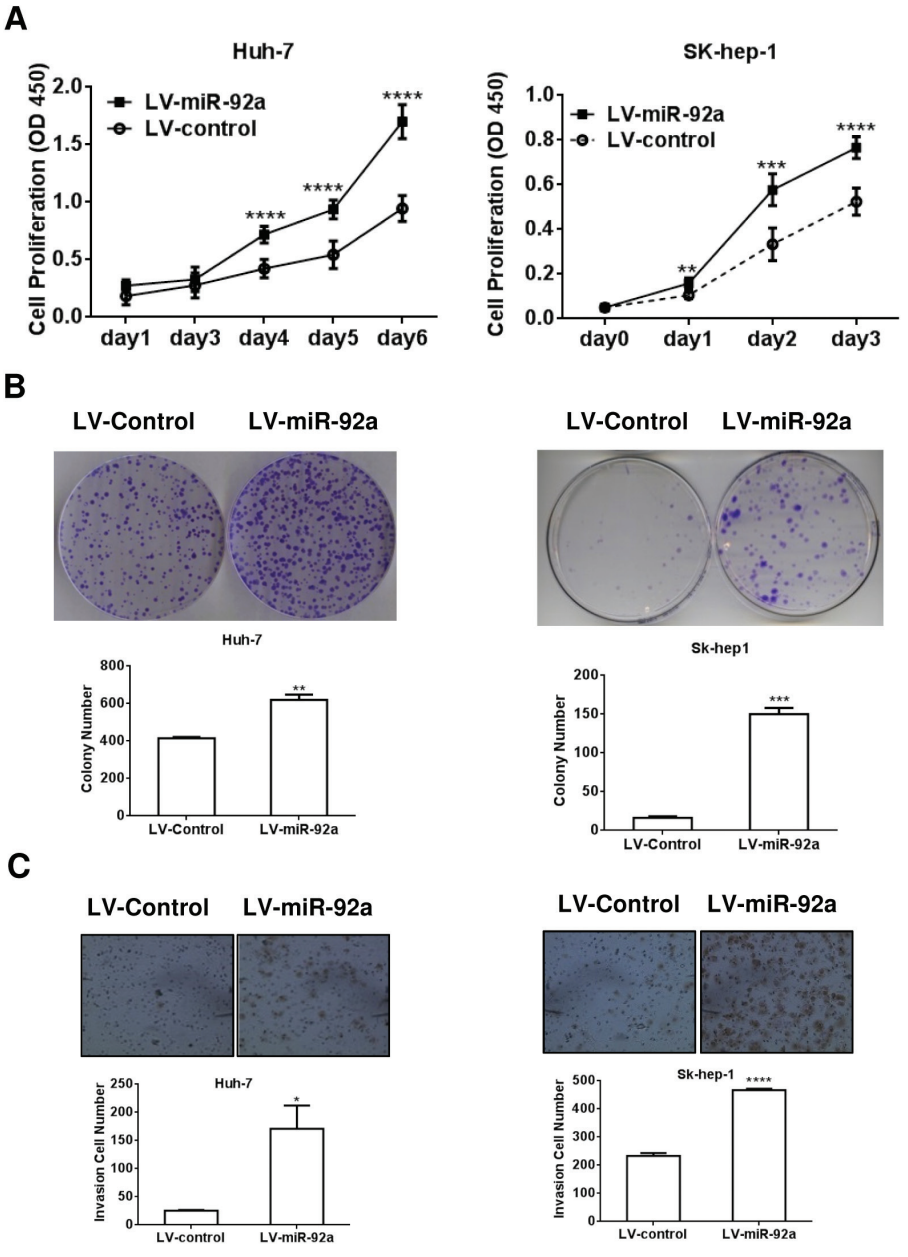

Figure 5. MiR-92a promotes HCC cell growths *in vitro*. Human HCC cells (Huh-7 and Sk-Hep-1) were infected with miR-92a lentivirus and miRNA scrambled control lentivirus, respectively. The stably transduced cells were analyzed for proliferation, colonogenic potential and invasion ability. (**A**) MiR-92a over-expression promotes HCC cell growth. Cell growth curves of human HCC cells (Huh-7 and Sk-Hep-1) stably transduced with miR-92a lentivirus (indicated as LV-miR-92a) or scrambled control (indicated as LV-control) (**$P < 0.01$, ***$P < 0.001$, ****$P < 0.0001$). (**B**) MiR-92a overexpression enhances HCC cell colony formation. The numbers of colonies were counted after 14 days. (*Upper panel*) Representative images showing colonies formed in cell culture dishes. (*Lower panel*) Average colony formation efficiency (the data are presented as mean ± SEM, **$P < 0.01$, ***$P < 0.001$). (**C**) MiR-92a overexpression promotes HCC cell invasion. (*Upper panel*) Representative images showing migrated cells (hematoxylin staining). (*Lower panel*) Average numbers of the invaded cells (the data are presented as mean ± SEM, *$P < 0.05$, ****$P < 0.0001$).

of the patients into two groups (low and high) according to each gene's expression level, and draw survival curve for each group. We observed a significant difference in survival curve between the two groups for the CREBL2 gene: the CREBL2-low group has a shorter patient survival time than the CREBL2-high group (Figure 6E) [$P < 0.05$, Log-rank (Mantel–Cox) test].

Discussion

MicroRNAs have been reported to be involved in HCCs (29–31). In the current study, we evaluated the role of the miR-17-92 cluster in hepatocellular cancer by using complementary approaches of tumor induction in mice, human hepatocellular cancer cell studies *in vitro*, and patient tissue analyses. We observed that target overexpression of the miR-17-92 cluster in the liver enhanced hepatic carcinogen-induced liver tumor development, characterized by more tumor number, larger tumor size and higher tumor volume. These *in vivo* findings are corroborated by the *in vitro* studies showing that forced overexpression of the miR-17-92 cluster (or one of its members, miR-92a) enhanced hepatocellular cancer cell proliferation, colony formation and invasiveness, *in vitro*. We further observed that inhibition of miR-17-92 cluster prevented hepatocellular cancer cell growth. These findings establish a key tumor-promoting role of

A

miRNA	Target	Correlation
hsa-mir-18a	CREBL2	-0.57633
hsa-mir-18a	EXPH5	-0.55797
hsa-mir-17	NTN4	-0.55385
hsa-mir-18a	MYLK	-0.54585
hsa-mir-17	PRRG1	-0.53791
hsa-mir-20a	PRRG1	-0.51822
hsa-mir-20a	NTN4	-0.51546
hsa-mir-18a	ESR1	-0.51213

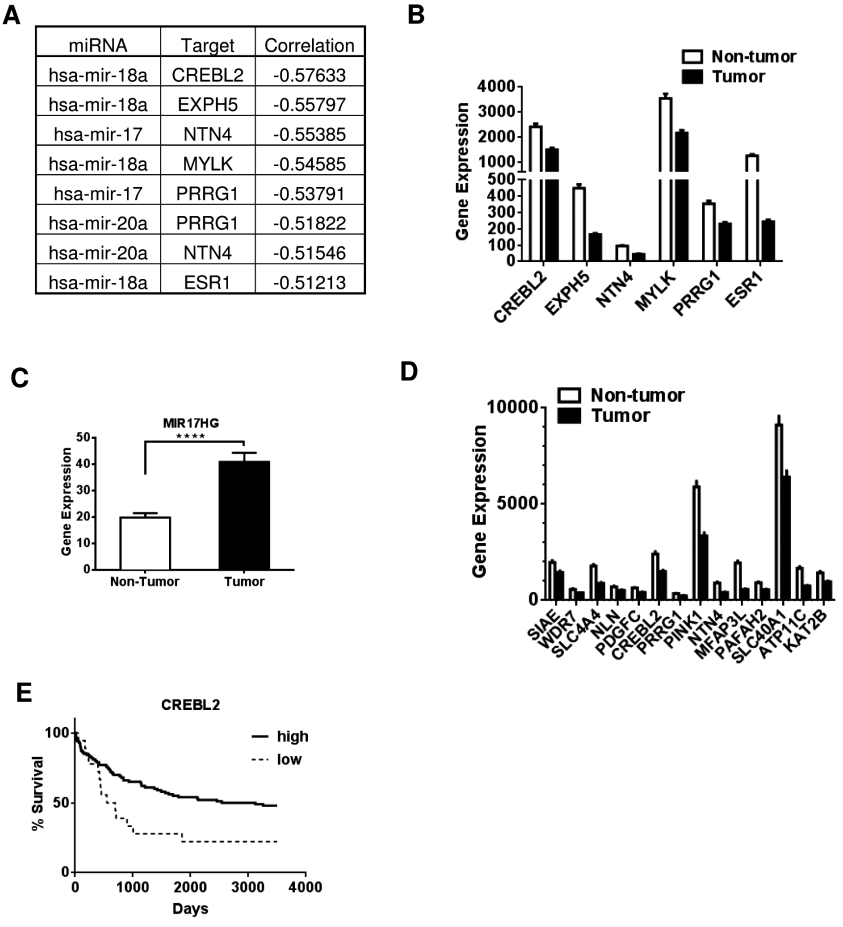

Figure 6. RNA-seq analysis of HCC patients data. (**A**) Correlation analysis of possible miR-target pairs for miR-17-92 cluster in human HCC and non-tumorous liver tissue samples (Pearson Corrletion, $P < 0.0001$). (**B**) Expression of target genes in human HCC and non-tumorous liver tissues (fold change>2.0, $P < 0.05$, *t*-test for each gene). (**C**) Average MIR17HG expression in human HCC and non-tumorous liver tissue samples. ****$P < 0.0001$. (**D**) The expression of negatively correlated genes with MIR17HG in human HCC and non-tumorous liver tissues (fold change > 1.5, $P < 0.05$, Pearson Correlation, and *t* test for each gene). (**E**) Survival curve of low and high groups of CREBL2 gene [$P < 0.05$, Log-rank (Mantel–Cox) test].

miR-17-92 cluster in hepatocarcinogenesis. The observation that target overexpression of miR-17-92 cluster in the liver enhances tumor development only in the setting of DEN treatment (but not spontaneously) suggests that the miR 17-92 polycistron is a tumor promoter but not a tumor initiator.

By taking advantage of the available online database (TCGA), we analyzed the mRNA and miRNA sequencing data from HCC patients. RNA-sequencing is a robust approach to quantify overall gene expression level, which provides high quality and reproducible data. Our analysis revealed that several miRNA-targets pairs, including miR-18a—CREBL2, miR-17—NTN4, miR-17—PRRG1, are probably important in hepatocarcinogenesis. We observed that the expression of one of these targets, CREBL2, is positively correlated with patients' survival. These findings suggest that miR-17-92 cluster may enhance hepatocarcinogenesis by downregulating key targets including CREBL2. In this context, it is worth mentioning that CREBL2 (cAMP-response-element-binding protein-like 2) is a CREB family member which can interact with CREB to regulate lipogenesis (32) and that CREBL2 may be a tumor suppressor as it is frequently deleted in malignancy (33).

Connolly *et al.* (34) reported increased expression of miR-17-92 cluster and miR-21 in hepatitis B virus-positive human and woodchuck HCCs. In this context, it is interesting that miR-17-92 is known to act with c-myc to promote carcinogenesis (12) and that c-myc can be activated by Hepatitis B virus X (35). Thus, miR-17-92 cluster may regulate carcinogenesis through interaction with other signaling molecules. Additionally, given that miR-21 is known to promote HCC through mechanisms including targeting PTEN, PDCD4, RHOB and other tumor suppressors (36–39) and that miR-21 is the most overexpressed miRNA in HCC patients (Supplementary Table 1, available at *Carcinogenesis* Online), it is possible that miR-17-92 and miR-21 may coordinately regulate hepatic carcinogenesis.

A recent study shows that miR-17-92 expression in HCC is regulated by epigenetic modification via histone deacetylation (40). Given that E2F1 and c-myc are well known to transcriptionally activate miR-17-92 cluster (41,42), it is possible that these transcription factors may also be implicated in regulating miR-17-92 expression in HCC. Thus, multiple mechanisms are probably to be involved for upregulation of miR-17-92 during hepatocarcinogenesis.

Recent studies suggest that circulating miRNAs, such as miR-21 and miR-122, may serve as biomarkers for HCC (43,44). Zhou *et al.* (45) showed that seven miRNAs set (miR-21, miR-26a, miR-27a, miR-122, miR-192, miR-223 and miR-801) can differentiate HCC form healthy, chronic hepatitis B and cirrhosis groups. miR-92a and miR-18a are also implicated in HCC (21,46,47). Given that miR-17-92 cluster, particularly miR-92a, is highly expressed in HCC as shown in the current study, future studies are needed

to validate whether miR-17-92 cluster or miR-92a can be used as a valid marker for early diagnosis of HCC. Moreover, given the oncogenic role of the miR-17-92 cluster in HCC as documented in the current study, further investigations are warranted to determine whether miR-17-92 can be targeted for future treatment of human HCC.

Supplementary material

Supplementary Tables 1–4 and Figures 1 and 2 can be found at http://carcin.oxfordjournals.org/

Funding

NIH (R01 CA102325).
Conflict of Interest Statement: None declared.

References

1. Llovet, J.M. et al. (2003) Hepatocellular carcinoma. Lancet, 362, 1907–1917.
2. Forner, A. et al. (2012) Hepatocellular carcinoma. Lancet, 379, 1245–1255.
3. El-Serag, H.B. (2011) Hepatocellular carcinoma. N. Engl. J. Med., 365, 1118–1127.
4. Farazi, P.A. et al. (2006) Hepatocellular carcinoma pathogenesis: from genes to environment. Nat. Rev. Cancer, 6, 674–687.
5. Bruix, J. et al.; American Association for the Study of Liver Diseases. (2011) Management of hepatocellular carcinoma: an update. Hepatology, 53, 1020–1022.
6. Filipowicz, W. et al. (2008) Mechanisms of post-transcriptional regulation by microRNAs: are the answers in sight? Nat. Rev. Genet., 9, 102–114.
7. Ambros, V. (2004) The functions of animal microRNAs. Nature, 431, 350–355.
8. Lewis, B.P. et al. (2003) Prediction of mammalian microRNA targets. Cell, 115, 787–798.
9. Cho, W.C. (2010) MicroRNAs: potential biomarkers for cancer diagnosis, prognosis and targets for therapy. Int. J. Biochem. Cell Biol., 42, 1273–1281.
10. Hayes, J. et al. (2014) MicroRNAs in cancer: biomarkers, functions and therapy. Trends Mol. Med., 20, 460–469.
11. He, B. et al. (2012) The association between four genetic variants in microRNAs (rs11614913, rs2910164, rs3746444, rs2292832) and cancer risk: evidence from published studies. PLoS One, 7, e49032.
12. He, L. et al. (2005) A microRNA polycistron as a potential human oncogene. Nature, 435, 828–833.
13. Bonauer, A. et al. (2009) The microRNA-17-92 cluster: still a miRacle? Cell Cycle, 8, 3866–3873.
14. Ota, A. et al. (2004) Identification and characterization of a novel gene, C13orf25, as a target for 13q31-q32 amplification in malignant lymphoma. Cancer Res., 64, 3087–3095.
15. Hayashita, Y. et al. (2005) A polycistronic microRNA cluster, miR-17-92, is overexpressed in human lung cancers and enhances cell proliferation. Cancer Res., 65, 9628–9632.
16. Tsuchida, A. et al. (2011) miR-92 is a key oncogenic component of the miR-17-92 cluster in colon cancer. Cancer Sci., 102, 2264–2271.
17. Chow, T.F. et al. (2010) The miR-17-92 cluster is over expressed in and has an oncogenic effect on renal cell carcinoma. J. Urol., 183, 743–751.
18. Si, H. et al. (2013) Circulating microRNA-92a and microRNA-21 as novel minimally invasive biomarkers for primary breast cancer. J. Cancer Res. Clin. Oncol., 139, 223–229.
19. Liu, G.H. et al. (2013) Serum miR-21 and miR-92a as biomarkers in the diagnosis and prognosis of colorectal cancer. Tumour Biol., 34, 2175–2181.
20. Zhu, H. et al. (2014) miR-17-92 cluster promotes cholangiocarcinoma growth: evidence for PTEN as downstream target and IL-6/Stat3 as upstream activator. Am. J. Pathol., 184, 2828–2839.
21. Shigoka, M. et al. (2010) Deregulation of miR-92a expression is implicated in hepatocellular carcinoma development. Pathol. Int., 60, 351–357.
22. Adams, E.J. et al. (1999) Comparison of different scoring systems for immunohistochemical staining. J. Clin. Pathol., 52, 75–77.
23. Verna, L. et al. (1996) N-nitrosodiethylamine mechanistic data and risk assessment: bioactivation, DNA-adduct formation, mutagenicity, and tumor initiation. Pharmacol. Ther., 71, 57–81.
24. Lewis, B.P. et al. (2005) Conserved seed pairing, often flanked by adenosines, indicates that thousands of human genes are microRNA targets. Cell, 120, 15–20.
25. Grün, D. et al. (2005) microRNA target predictions across seven Drosophila species and comparison to mammalian targets. PLoS Comput. Biol., 1, e13.
26. Chen, K. et al. (2006) Natural selection on human microRNA binding sites inferred from SNP data. Nat. Genet., 38, 1452–1456.
27. Anders, G. et al. (2012) doRiNA: a database of RNA interactions in post-transcriptional regulation. Nucleic Acids Res., 40, D180–D186.
28. Enright, A.J. et al. (2003) MicroRNA targets in Drosophila. Genome Biol., 5, R1.
29. D'Anzeo, M. et al. (2014) The role of micro-RNAs in hepatocellular carcinoma: from molecular biology to treatment. Molecules, 19, 6393–6406.
30. Chen, Y. et al. (2014) MicroRNAs: the fine modulators of liver development and function. Liver Int., 34, 976–990.
31. Xu, Y. et al. (2013) Three common functional polymorphisms in microRNA encoding genes in the susceptibility to hepatocellular carcinoma: a systematic review and meta-analysis. Gene, 527, 584–593.
32. Ma, X. et al. (2011) CREBL2, interacting with CREB, induces adipogenesis in 3T3-L1 adipocytes. Biochem. J., 439, 27–38.
33. Hoornaert, I. et al. (1998) CREBL2, a novel transcript from the chromosome 12 region flanked by ETV6 and CDKN1B. Genomics, 51, 154–157.
34. Connolly, E. et al. (2008) Elevated expression of the miR-17-92 polycistron and miR-21 in hepadnavirus-associated hepatocellular carcinoma contributes to the malignant phenotype. Am. J. Pathol., 173, 856–864.
35. Terradillos, O. et al. (1997) The hepatitis B virus X gene potentiates c-myc-induced liver oncogenesis in transgenic mice. Oncogene, 14, 395–404.
36. Bao, L. et al. (2013) MicroRNA-21 suppresses PTEN and hSulf-1 expression and promotes hepatocellular carcinoma progression through AKT/ERK pathways. Cancer Lett., 337, 226–236.
37. Zhu, Q. et al. (2012) miR-21 promotes migration and invasion by the miR-21-PDCD4-AP-1 feedback loop in human hepatocellular carcinoma. Oncol. Rep., 27, 1660–1668.
38. Qiu, X. et al. (2013) HBx-mediated miR-21 upregulation represses tumor-suppressor function of PDCD4 in hepatocellular carcinoma. Oncogene, 32, 3296–3305.
39. Connolly, E.C. et al. (2010) Overexpression of miR-21 promotes an *in vitro* metastatic phenotype by targeting the tumor suppressor RHOB. Mol. Cancer Res., 8, 691–700.
40. Yang, H. et al. (2015) Histone deacetylase inhibitor SAHA epigenetically regulates miR-17-92 cluster and MCM7 to upregulate MICA expression in hepatoma. Br. J. Cancer, 112, 112–121.
41. Aguda, B.D. et al. (2008) MicroRNA regulation of a cancer network: consequences of the feedback loops involving miR-17-92, E2F, and Myc. Proc. Natl. Acad. Sci. USA, 105, 19678–19683.
42. O'Donnell, K.A. et al. (2005) c-Myc-regulated microRNAs modulate E2F1 expression. Nature, 435, 839–843.
43. Qi, P. et al. (2011) Serum microRNAs as biomarkers for hepatocellular carcinoma in Chinese patients with chronic hepatitis B virus infection. PLoS One, 6, e28486.
44. Petrini, E. et al. (2015) MicroRNAs in HBV-related hepatocellular carcinoma: functions and potential clinical applications. Panminerva Med. 21 April 2015. [Epub ahead of print]. Med. ISSN 0031-0808. Online ISSN 1827-1898.
45. Zhou, J. et al. (2011) Plasma microRNA panel to diagnose hepatitis B virus-related hepatocellular carcinoma. J. Clin. Oncol., 29, 4781–4788.
46. Shen, J. et al. (2015) Genome-wide expression of MicroRNAs is regulated by DNA methylation in hepatocarcinogenesis. Gastroenterol. Res. Pract., 2015, 230642.
47. He, S. et al. (2015) MicroRNAs as biomarkers for hepatocellular carcinoma diagnosis and prognosis. Clin Res Hepatol Gastroenterol. 3 March 2015. [Epub ahead of print]. pii: S2210-7401(15)00034-0. doi: 10.1016/j.clinre.2015.01.006.